

Oxide Ion Conductivity of Mechanically produced Calcia Stabilised Zirconia for Oxygen Sensing Applications

M. Kannan^{a*} , Satyendra Singh^b, R.R. Prasad^c

^aUttarakhand Technical University, Research Scholar-Mechanical Engineering, Dehradun, India.

^bBipin Tripathi Kumaon Institute of Technology (BTKIT), Mechanical Engineering Department, Dwarahat, India.

^cBSM College of Engineering, Roorkee, India.

Received: February 21, 2022; Revised: August 05, 2022; Accepted: September 17, 2022

Cryo-milling was used to make calcia stabilized zirconia (CSZ) powders with 9 mol%, 12 mol%, and 15 mol% of calcia. Powder X-ray diffraction was done to examine the phase growth in prepared powders over the course of 80h of mechanical alloying (MA) in cryogenic environment at 300rpm. The calcined powders were hydraulically pressed into cylindrical shaped sensor elements in a uniaxial press and then sintered for 4h at 1400°C. The microstructure of sintered pellets were studied using Scanning Electron Microscope (SEM). Electrical Conductivity measurements of the prepared stabilized zirconia at various temperatures over a temperature range of 200°C to 500°C using a dual-probe impedance analyzer is carried out and the effects of composition and temperature on the grain boundary impedance of CSZ were analyzed. Conductivity is discussed in terms of ionic vacancies in the bulk due to calcium ion substitution and available grain boundary paths. Ionic Conductivity of prepared CSZ is compared for suitability in oxygen sensing applications.

Keywords: *Calcia-Stabilized Zirconia, Conductivity, Mechanical Alloying, Cryo-Milling.*

1. Introduction

Zirconia, one of the most promising ceramics, has been extensively studied due to its favorable structural, biocompatibility and electrical properties that make it suitable for dental and oxygen sensing applications^{1,2}. At normal temperature, pure zirconium dioxide exhibits a monoclinic crystal structure. However, as the temperature rises from ambient temperature to the melting point, its structure shifts from tetragonal to cubic³. Large stresses are created during the phase transition from cubic to tetragonal to monoclinic, causing purer zirconium dioxide to break when cooled from a high temperature⁴. Various oxides of Magnesia, yttria, calcia or ceria in variable proportions are added to stabilize the tetragonal and or cubic phases⁵. The tetragonal phase in zirconia can be metastable in some instances, and if enough of this metastable phase is present, the tetragonal phase can change to monoclinic phase, causing volume expansion. The crack can be compressed as a result of the phase change to monoclinic, which slows its growth and increases fracture toughness. The toughening due to transformation of stabilized zirconia boosts their reliability and longevity dramatically⁶. Tetragonal zirconia polycrystalline (TZP) is a unique type of zirconia with a polycrystalline structure made up entirely of the metastable tetragonal phase⁷.

The stabilised zirconia ceramics are utilized to find the content of oxygen using oxygen measuring devices in gases, combustion engine exhaust gases and in solid oxide fuel cells as it has high oxygen conductivity. They have long

been applied as a sensor to boost combustion efficiency⁸. The extreme susceptibility of fully stabilized zirconia (FSZ) to thermal shock is a severe concern in electrochemical cells, which is resolved by using partially stabilized zirconia (PSZ) cells⁹. To utilize the potential of zirconia ceramics, its stabilization to retain the phase and enhanced properties due to transformation toughening many approaches to obtain stabilized zirconia powders have been researched¹⁰. Sol-gel¹¹, spray pyrolysis¹², precipitation routes¹³, and rapid combustion routes¹⁴ are the most effective chemical techniques.

A new cryochemical technique to produce nanosized CSZ precursor powders involving coprecipitation and freeze drying has been studied¹⁵. Though these techniques provide purest powders, effort involved is relatively higher than the solid state or mechanical alloying route, and with usage of calcia instead of yttria or ceria for stabilization, cost is reduced. Type of Sintering and sintering conditions of green pellets influence the properties¹⁶. Few properties like Vickers micro-hardness, fracture toughness are influenced by grain size. Hardness increases while fracture toughness decreases with a decreasing grain size^{17,18}. When the grain size increases, stability of zirconia reduces and becomes more open to spontaneous tetragonal-to-monoclinic phase transformations ending with lesser strength gradually¹⁹. The composition of the stabilizers and grain boundaries affect the conductivity of zirconia stabilized with yttria and calcia and by adjusting the composition of the stabilizers and examining the microstructure of the grain boundaries, it could provide good ionic conductivity with low-cost stabilized zirconia²⁰.

*email: mkananm@gmail.com

In this work, high-energy ball milling was carried out to produce submicron to nano-grained size, calcia stabilized zirconia powder by using commercial calcium oxide and zirconium oxide powders. The sintering of different mol fractions of calcia stabilized zirconia after mechanical alloying in a liquid nitrogen environment, i.e., cryo-milling, was carried out. Microstructural studies and resistivity behaviors of three compositions of calcia stabilized zirconia system are studied for suitability in oxygen sensing applications.

2. Experimental Procedure

Calcium oxide (CaO) (average particle size: 10 μm) and Zirconium oxide (ZrO_2) (average particle size: 5 μm) powders obtained from Sigma Aldrich were mixed to make three distinct compositions. The powder proportions were weighed to get 9 mol percent calcia, 12 mol percent calcia, and 15 mol percent calcia, with zirconia as the matrix component. Before attaching to the planetary ball mill, the weighted powder mixtures of each constituent were loaded and sealed in zirconium steel jars of 500 mL, in addition with liquid nitrogen (Retsch Company) and grinding media. All studies employed about 40 zirconium steel balls weighing 15 grams apiece, with a mass ratio of 10:1 steel balls to powder. The three components were placed in separate jars, with the powder and grinding medium occupying less than 1/3 of overall volume and running at 300 rpm for 80 hrs with short interval gaps.

The milled samples were analyzed in the 2- θ range 20°-80° at a speed of 1° per minute utilising X-ray Diffraction (D8-Advance, Bruker AXS) under Cu-K α radiation. Scanning electron microscopy (SEM) was used to investigate the powder sample (SEM; Quanta 200 FEG, FEI). For sintering, green pellets were made from all the three compositions after 80 hours of milling with liquid nitrogen. Before compacting with 13 tonnes of compaction pressure to make cylindrical pellets under the uniaxial pressing machine, about 20g of prepared powder was rigorously combined with Poly Vinyl Alcohol (PVA) binder 3 wt percent. Stearic acid was applied on the die as a lubricant. Green samples were sintered for 4 hours in a muffle furnace at 1400°C. Cracking is avoided by maintaining constant heating, cooling speeds of 5°C/min. The furnace was allowed to cool down naturally for 24 hours, and then the sample was removed.

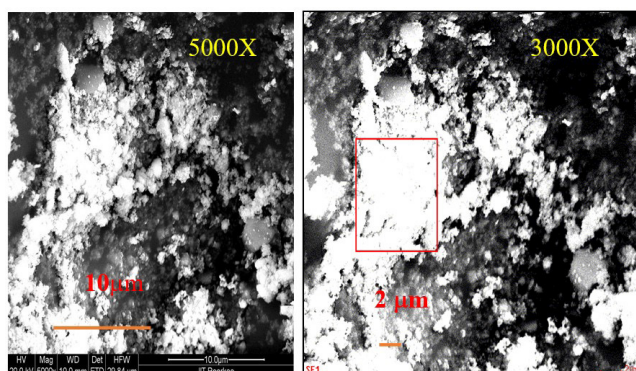
Apparent sintered density is calculated by liquid displacement technique and by mass volume relationship. Scanning electron microscope (SEM) studies are carried to know how the surface of the pellets looked, after sintering. Because the system is not conductive at ambient temperature, the samples were gold plated. Two surfaces of each sintered sample were polished using abrasive paper, and silver paste was spread to the samples on both surfaces before being thermally treated at 150°C for 30 minutes at a speed of 3°C/min. A 2- probe sample holder was employed for analyzing impedance, and the sample holder was kept in a tube furnace. At temperatures of 500 °C, 400 °C, 450 °C, 300 °C, and 200 °C using impedance analyser, impedance is determined with air as a media in the range of 10² -10⁶ Hz frequency from 150°C to 500°C. The HIOKI 3532-50 LCR HiTester gives the data by the help of software. At the tested temperatures, the ionic conductivity of each of the compositions was determined.

3. Result and Discussion

A planetary ball mill was used to mill the powders that were weighed for each composition and operated in a cryogenic environment. Cryo-milling is to decrease bigger particle sizes to nanoscale, resulting in improved conductivity and the two ingredient powders mechanically alloyed together. SEM and XRD studies are carried out to know the maximum size range of the grains (crystallite) in the powder sample prepared.

SEM micrographs and EDS map of calcia- stabilized zirconia powder are shown in Figures 1-3 taken at 5000X magnification for knowing the grain (crystallite) size and morphology of powder. Agglomeration in powders was seen in given figure. For all of the powders, the average agglomeration size was less than 1 μm . The majority of the particles have a spherical shape, with only a small percentage having a hollow or irregular shape. The average grain size of powder created by this approach is about 22 nm in all circumstances, which is an important attribute.

Figures (1-3) indicate the agglomerate size and composition of CaO, ZrO. The figures are the EDX photographs showing clearly the zirconia phase and calcia phase. This EDX have taken at various locations randomly for knowing the compositions of calcia and zirconia.

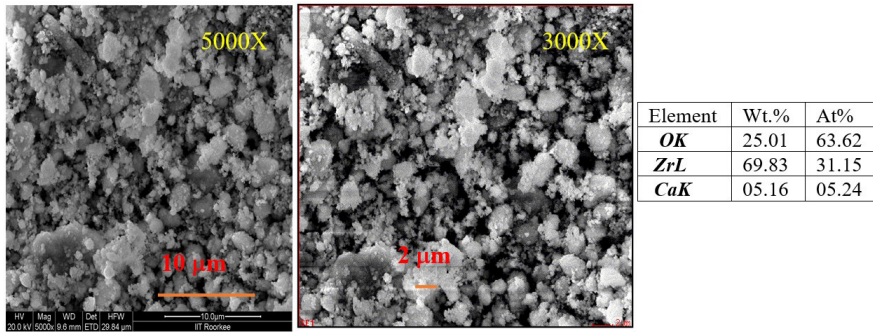
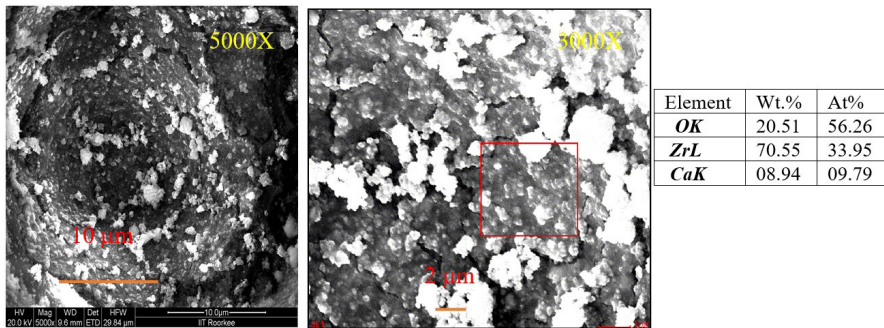


Element	Wt.%	At%
OK	31.28	71.14
ZrL	65.88	26.28
CaK	02.85	02.58

Figure 1. SEM and EDS analysis for 9 mol % CaO powder sample.

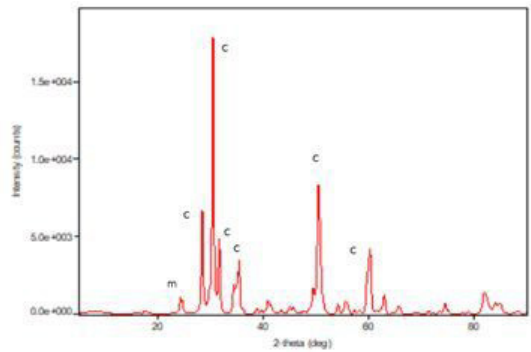
Table 1. XRD measurements of grain size in nanometers for samples.

CaO μm	ZrO ₂ μm	9mol% (80hrs) nm	12mol% (80hrs) nm	15mol% (80hrs) nm
10	5	21.07	21.69	22.15

**Figure 2.** SEM and EDS analysis for 12 mol % CaO powder sample.**Figure 3.** SEM and EDS analysis for 15 mol % CaO powder sample.

After the 80h were completed, samples were collected and sent for XRD whose plots were used to determine grain size using Scherer's Formula²⁰ Table 1. Sums up the grain size calculated for all the samples.

Figure 4 shows XRD pattern of the ZrO₂-15 mol% CaO. Peaks obtained in XRD pattern indicates phases of the powders obtained. The powder pattern, obtained for the 9-15 mol% CaO solid solution composition, exhibits the main reflection due to the cubic phase. Because the XRD Method is studied at the crystal level and is based on the separation distance in a crystal between 2 planes, the size indicated by Scherer's Formula correlates to the finer grains²¹. Also, the average grain size of all samples is ranging between 21 and 22 nm. By comparing, the d values of the peaks in the XRD plots, the existence of the zirconia in cubic phase may be conclusively established which in turn confirms that some zirconia ions have been replaced with calcium ions, causing oxygen vacancies to develop. EDS testing reveals that all constituents are present and in all phases and since MA is done using ball milling presence of impurities is expected. Hence, smaller peaks are ignored as noise²². Density calculated using liquid displacement technique based on Archimedes principle is around 5.21g/cm³ and when compared with theoretical density from literature of 5.52g/cm³ densification is significantly achieved with less porosity. Percentage change seen in the apparent values of

**Figure 4.** Calcia-stabilized zirconia powder XRD with 15 Mol% CaO for 80 hours.

density obtained from mass-volume relationship is around 40% increase due to shrinkage during sintering as shown in Table 2. Average densification obtained is around 92% of theoretical density, which relates to presence of less porous and coarse grains in the microstructure²³.

Figure 5-7 shows the SEM and EDS maps for the material sintered at 1400°C for 4 hours with 9-15 mol% CaO. According to the EDS map, all of the samples possessed consistent Zr and Ca component distribution in microstructure. A tiny fraction

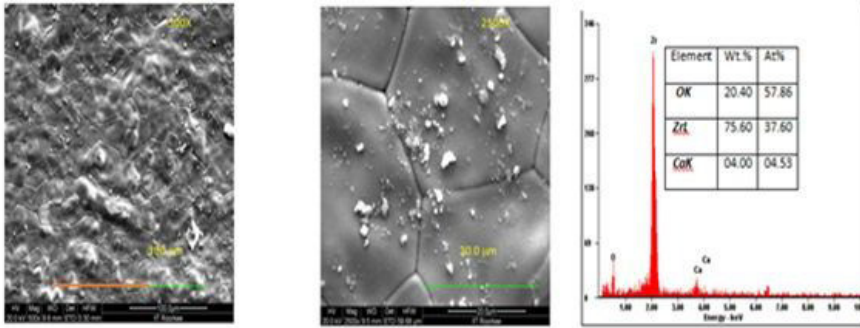


Figure 5. SEM and EDS analysis of CSZ with 9 mol% CaO.

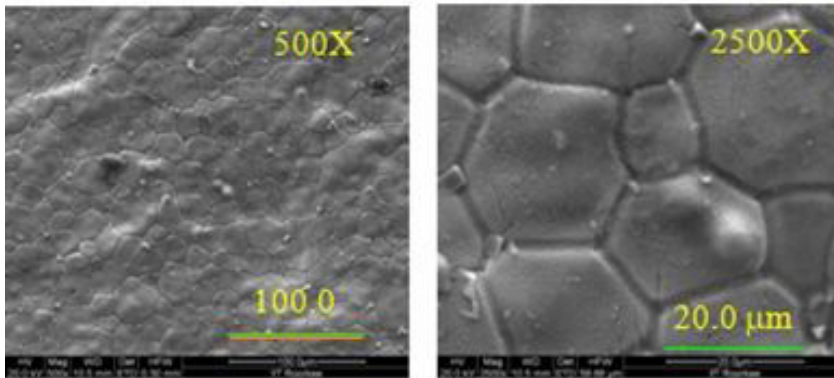


Figure 6. SEM and EDS analysis of CSZ with 12 mol% CaO.

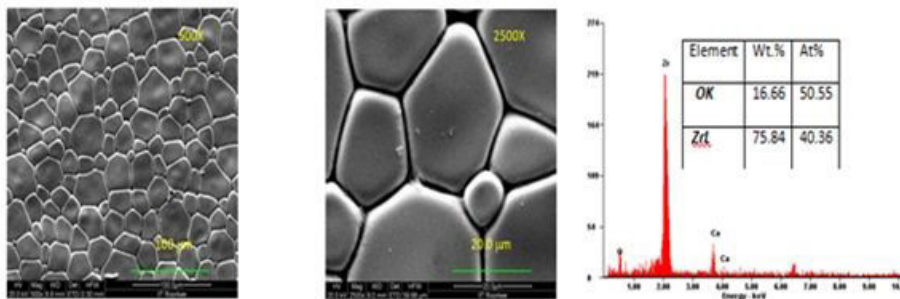


Figure 7. SEM and EDS analysis of CSZ with 15 mol% CaO.

Table 2. Density measurements.

Mol %	Density before sintering (g/cm ³)	Density after sintering(g/cm ³)	% change
9	3.55	5.21	46
12	3.51	5.11	45
15	3.68	5.19	41

of pores maybe seen in the matrix (Figure 6). The sample has a significant quantity of CaO dispersed inside the matrix, mostly at the grain boundaries, as seen in the EDS maps. The solubility limits of calcia in cubic zirconia have been determined to be 9-15 mol percent when sintered at 1400°C. This explains why zirconia powder containing 15 mol% CaO

in the raw powder has a better defined microstructure and a more uniform element distribution^{24,25}.

Figures 8-10 show the results of impedance experiments at various temperatures for samples containing 12 mol % CaO, 15 mol% CaO, and 9 mol% CaO. The results are determined using the basic Rs (C-Rp) model. Table 3 shows that when testing temperatures rise, the low frequency intersection of the semicircle, which reflects the total of bulk (i.e. grain interiors, R_b) and internal interface resistance (pores and grain-boundary resistance, R_{gb}) decreases for all materials^{26,27}.

For studying the electrical characteristics of solid electrolytes, the complex impedance approach is highly useful. In comparison to the Rs (C-Rp) model, this is a simple method. When AC data is displayed on complex impedance charts, the results are Z'

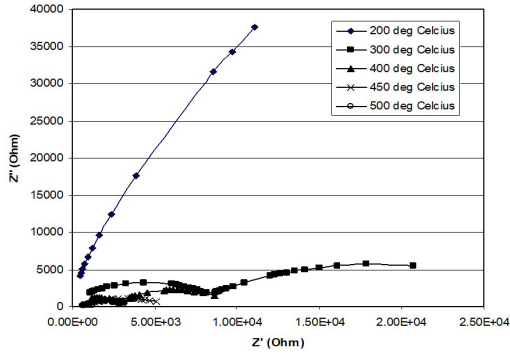


Figure 8. Complex impedance measured at 200,300,400,450 and 500°C in air of CSZ specimen containing 12 mol% CaO.

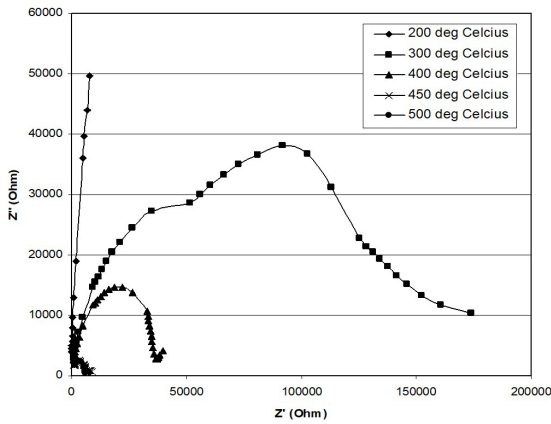


Figure 9. Complex impedance measured at 200,300,400,450 and 500°C in air of CSZ specimen containing 15 mol % CaO.

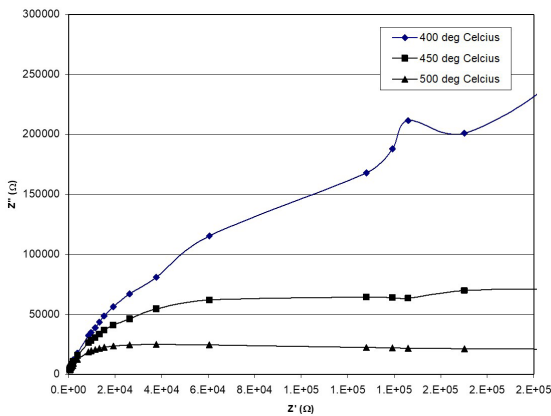


Figure 10. Complex impedance measured at 400,450 and 500°C in air of CSZ specimen containing 9 mol% CaO.

versus Z'' , where Z' and Z'' are the complex impedance's real and virtual components. The electrode effect, grain-boundary effect, and lattice effect, in that sequence, cause arcs 1, 2, and 3 with increased frequency²⁸.

Table 3. Pellet area and length of CSZ.

Composition	9 mol%	12mol%	15 mol%
Pellet area	0.8996 cm ²	0.89285cm ²	0.77321cm ²
Pellet length	0.208 cm	0.19466 cm	0.18 cm

Conductivity mechanism is studied by separating the effects of bulk and grain boundary resistivity. From Figure 11, we see that total (bulk and grain-boundary) resistance:

$$(R) = R_b + R_{gb} \quad (1)$$

with the arcs referring to lattice (bulk) behavior and grain boundary effect. Figure suggests that with increase in calcia content, conductivity increases^{29,30}.

The conductivity was measured using the 2- probe method. The silver paste applied at both the surfaces acted as contact points for the surfaces. The impedance was measured at temperatures of 200°C, 300°C, 400°C, 450°C, and 500°C, and the equipment gave the reading. With the help of given Equation 1, resistance is calculated. Table 3 enlists the pellet dimensions used for conductivity testing. Total resistance ($R_b + R_{gb}$) and resistivity of the 9, 12, and 15 mol % CSZ as shown in Table 4 and Table 5 are given below-

The conductivity obtained for different compositions was plotted with inverse of temperature (in degree Kelvin). The slope of this as explained in the literature survey gives the value of E_a/k . Hence, multiplying the slope by k , Boltzman constant, the value of Activation Energy, E_a in eV for different temperatures is obtained as well.

Table 6 illustrates the resistivity determined using the two probe approach for the various compositions. The change in log resistivity with composition in Table 6 confirms that the conductivity increases as the concentration of calcia ions in calcia stabilized zirconia increases^{24,27}. As a result, it is possible that increasing doping enhances conductivity. However, this is based on the expectation that all ions are mobile and contribute to conductivity. This is also dependent on the temperature. Arrhenius plots were used to investigate this effect. Figure 12 illustrates a linear trend in the \ln (conductivity) vs. $1/T$ graph for calcia stabilized zirconia. This suggests that the ions' mobility in the temperature range investigated, 573°K to 773°K, is governed by a consistent mechanism.

The activation energy in eV was estimated for the various compositions, as shown in Table 7. 0.4 -0.59 eV was calculated for 9-15 mol percent calcia stabilized zirconia in the range of 300°C to 500°C. This is lower than the value calculated in the range of 0.75 eV to 1.1 eV at temperatures ranging from 800°C to 1200°C²⁶.

The quantity of stabilizing cation in zirconia solid solutions is related to the electrical conductivity^{28,31}. Despite the fact that oxygen vacancy concentration rises with doping level, conductivity of zirconia solid solution increases with concentration regardless of cation charge until stability of cubic zirconia is achieved fully. Vacancy interactions or the creation of vacancy clusters, vacancy ordering, or the

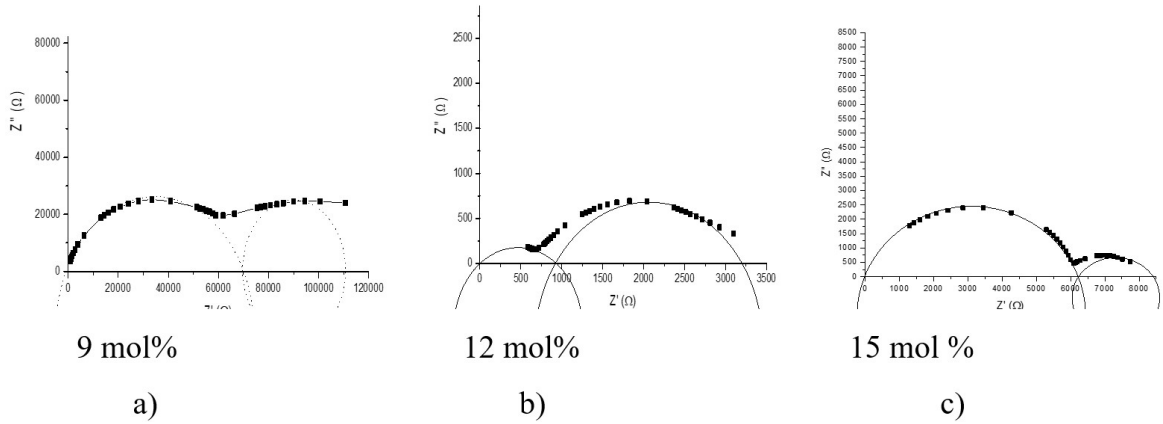


Figure 11. Complex impedance plots at 500°C for three samples with CaO a) 9 Mol % b) 12 mol % c) 15 mol%.

Table 4. Total (bulk and grain-boundary) resistance of the 9, 12, 15 mol% CSZ.

Temperature °C	200°C	300°C	400°C	450°C	500°C
9 mol% CaO	-	2.06×10^6	1.30×10^6	2.95×10^5	1.10×10^5
$R_b + R_{gb}$ (Ω)					
12 mol% CaO	2.48×10^6	2.21×10^4	9.09×10^3	5.03×10^3	3.20×10^3
$R_b + R_{gb}$ (Ω)					
15 mol%	2.19×10^6	1.51×10^5	3.50×10^4	1.00×10^4	8.42×10^3
$R_b + R_{gb}$ (Ω)					

emergence of a second phase are all possible causes for this behavior^{29,32}.

A possible inference from the above results could be that the conductivity in calcia stabilized zirconia at lower temperatures is governed by the grain boundary diffusion. This has lower activation energy, since the compact lattice organization is absent at the grain boundaries. Hence, resulting in easier diffusion paths and subsequently higher conductivity. In bulk/lattice diffusion, the atoms are tightly bonded to each other due to attractive forces and there is a very narrow gap for the ions to diffuse across. This causes the activation energy to be higher and conductivity suffers²⁸. Response characteristics to the oxygen environment by the CSZ samples with different compositions studied by Zhou and Ahmad⁸ shows that ion conductivity is related to oxygen sensing capabilities. For 15 mol% CaO composition prepared by Sol-Gel route at 700°C response was noted as quick and stable at various oxygen concentrations³³. Conductivity measured in CSZ sample prepared by MA route is comparably lesser but significant enough for sensing applications for analyzing content of oxygen in exhaust gases of engines²³. With increase in CaO content, oxide ion conductivity increases initially and then it gets lowered. Deviation from theoretical values is larger for higher concentration of CaO because of lower ion conductivity values indicated by the impedance analysis⁸.

Table 5. Resistivity of 3 compositions vs Temperature by Two Probe Method.

Temperature (°C)	9 mol% (ohm cm)	12 mol% (ohm cm)	15mol% (ohm cm)
200	-	1.14×10^6	9.40×10^6
300	8.89×10^6	1.02×10^5	6.50×10^5
400	5.65×10^6	4.17×10^4	1.50×10^5
450	1.27×10^6	2.31×10^4	4.32×10^4
500	4.79×10^5	1.47×10^4	3.62×10^4

Table 6. Log Resistivity of 3 compositions vs Temperature by Two Probe Method.

Temperature (°C)	9 mol% (ohm cm)	12 mol% (ohm cm)	15 mol% (ohm cm)
200	-	6.06	6.97
300	6.95	5.01	5.81
400	6.75	4.62	5.18
450	6.11	4.44	4.64
500	5.68	4.17	4.56

Table 7. Activation Energy measured from slope of above graphs in Ev.

9 mol%	12 mol%	15 mol%
0.55 eV	0.377 eV	0.593 eV

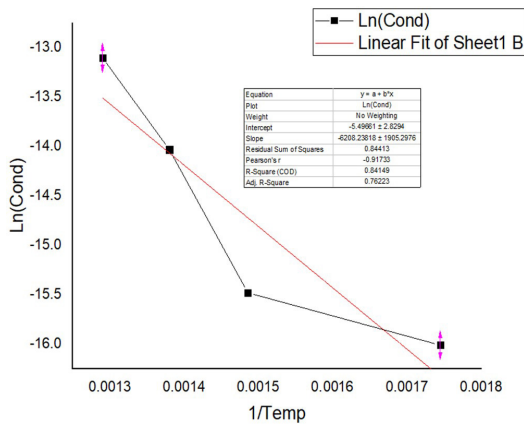


Figure 12. Arrhenius Plot for Composition 9 mol%.

4. Conclusion

In cryogenic circumstances, mechanical alloying using High Energy Ball Mill was employed to manufacture calcia-stabilized zirconia (CSZ) powders. Calcia-stabilized zirconia powders with cubic or tetragonal phase and 9, 12, and 15 mol% CaO composition was prepared. Sintering the green bodies at 1400°C for 4 hours generated a dense and well-defined microstructure. X-ray diffraction patterns confirmed the existence of the cubic phase and a very feeble trace of an undetermined phase in the 12 mol% CaO sample. Scanning of Field Emissions Electron microscopy demonstrates that along the matrix grain boundaries, a particular percentage of small grains with CaO in higher amounts was generated and dispersed. According to impedance study, the sensor cell with 9, 12 mol% CaO has much lower resistance than the one with 15 mol% CSZ.

The Arrhenius curves were plotted for different compositions and activation energy, in eV compared with literature, was calculated at these temperatures.

The important results can be summarized as follows:

- XRD validates the grain size of powders in the range 21 nm using Scherer's Formula.
- Linear relation between log resistivity and composition validates that as concentration of calcia ions in calcia stabilized zirconia increases, the conductivity increases.
- From 12-15 mol% calcia stabilized zirconia show a linear trend indicating a consistent mechanism governing the mobility of the ions in the temperature range being studied i.e. 573K to 773 K
- The value of activation energy for 12-15 mol% calcia stabilized zirconia was calculated ~0.4-.59 eV.
- Sensor elements prepared from powders obtained by MA route can be utilized for oxygen sensing applications and thus, reducing cost.

5. References

1. Ban S. Reliability and properties of core materials for all-ceramic dental restorations. *Jpn Dent Sci Rev.* 2008;44:3-21.
2. Jagannathan KP, Tiku SK, Ray HS, Ghosh A, Subbarao EC. Technological applications of solid electrolytes. In: Subbarao EC, editor. *Solid electrolytes and their applications.* New York: Plenum Press; 1980. p. 201-59
3. Garvie RC, Hannink RH, Pascoe RT. Ceramic steel? *Nature.* 1975;258:703-704.
4. Kisi EH, Howard CJ. Crystal structure of zirconia phases and their inter-relation. *Key Eng Mater.* 1998;153:1-36.
5. Shoja Razavi R, Loghman-Estark MR. Advance techniques for the synthesis of nanostructured zirconia-based ceramics for thermal barrier application. In: Mishra AK, editor. *Sol-gel based nanoceramic materials: preparation, properties and applications.* Cham: Springer; 2017. http://dx.doi.org/10.1007/978-3-319-49512-5_2
6. Guazzato M, Albakry M, Ringer SP, Swain MV. Strength, fracture toughness and microstructure of a selection of all-ceramic materials. PartII. Zirconia based dental ceramics. *Dent Mater.* 2004;20:449-56.
7. Kelly J, Denry I. Stabilized zirconia as a structural ceramic: an overview. *Dent Mater.* 2008;24(3):289-98. <http://dx.doi.org/10.1016/j.dental.2007.05.005>.
8. Zhou M, Ahmad A. Synthesis, processing and characterization of calcia-stabilized zirconia solid electrolytes for oxygen sensing applications. *Mater Res Bull.* 2006;41:690-6.
9. Lamas DG, Lascalea GE, Walsøe de Reca NE. Synthesis and characterization of nanocrystalline powders for partially stabilized zirconia ceramics. *J Eur Ceram Soc.* 1998;18(9):1217-21.
10. Kannan M, Singh S, Prasad RR. Synthetic methods to obtain calcia-stabilized zirconia powders: a review. In: Manik G, Kalia S, Sahoo SK, Sharma TK, Verma OP, editors. *Advances in mechanical engineering: lecture notes in mechanical engineering.* Singapore: Springer; 2021. p. 405-16. https://doi.org/10.1007/978-981-16-0942-8_39
11. Shukla AK, Sharma V, Dhas NA, Patil KC. Oxide-ion conductivity of calcia- and yttria-stabilized zirconias prepared by a rapid-combustion route. *Mater Sci Eng B.* 1996;40(2-3):153-7.
12. Mirosław M. Bućko, Ionic conductivity of CaO-Y2O3-ZrO2 materials with constant oxygen vacancy concentration. *J Eur Ceram Soc.* 2004;24(6):1305-8.
13. Gong J, Li Y, Tang Z, Zhang Z. Enhancement of the ionic conductivity of mixed calciaryttria stabilized zirconia. *Mater Lett.* 2000;46:115-9.
14. Ugorek M. A comparison of microstructure and electrical Properties of 8 mol% yttria stabilized zirconia Processed under conventional, microwave, and fast fire Sintering techniques [thesis]. Alfred, New York: Alfred University; 2004.
15. Kurapova OY, Nechaeva DV, Ivanov AV, Golubev SN, Ushakov VM, Konakov VG. Thermal evolution of the microstructure of calcia stabilized zirconia precursors manufactured by cryochemical technique. *Rev Adv Mater Sci.* 2016;47:95-104.
16. Dahl P, Kaus I, Zhao Z, Johnsson M, Nygren M, Wiik K, et al. Densification and properties of zirconia prepared by three different sintering techniques. *Ceram Int.* 2007;33:1603-10.
17. Sahin O, Demirkol I, Göcmez H, Tuncer M, Cetinkara HA, Güder HS, et al. Mechanical properties of nano crystalline tetragonal zirconia stabilized with CaO, MgO and Y2O3. *Acta Phys Pol A.* 2013;123(2):300.
18. Basu B. Toughening of yttria-stabilised tetragonal zirconia ceramics. *Int Mater Rev.* 2005;50(4):239-56.
19. Matsui K, Yoshida H, Ikuhara Y. Isothermal sintering effect on phase separation and grain growth in yttrium-stabilized tetragonal zirconia polycrystal. *J Am Ceram Soc.* 2009;92:467-75.
20. Li Y, Tang Z, Zhang Z, Gong J. Electrical conductivity of zirconia stabilized with yttria and calcia. *J Mater Sci Lett.* 1999;18:443-4.
21. Shukla S, Seal S. Phase stabilization in nanocrystalline zirconia. *Rev Adv Mater Sci.* 2003;5(2):117-20.
22. Maridurai T, Balaji D, Sagadevan S. Synthesis and characterization of yttrium stabilized zirconia nanoparticles. *Mater Res.* 2016;19(4):812-6.
23. Prasad RR, Daniel BS. Cryogenically synthesized mechanically alloyed calcia stabilized zirconia. *Adv Mat Res.* 2009;67:271-6.

24. Muccillo R, Buissa Netto RC, Muccillo ENS. Synthesis and characterization of calcia fully stabilized zirconia solid electrolytes. *Mater Lett*. 2001;49:197-201.
25. Ramírez-González J, West AR. Electrical properties of calcia-stabilised zirconia ceramics. *J Eur Ceram Soc*. 2020;40(15):5602-11. <http://dx.doi.org/10.1016/j.jeurceramsoc.2020.06.023>.
26. Kurapova OY, Glukharev AG, Glumov OV, Kurapov MY, Boltynjuk EV, Konakov VG. Structure and electrical properties of YSZ-rGO composites and YSZ ceramics, obtained from composite powder. *Electrochim Acta*. 2019;320:134573.
27. Kurapova OY, Glumov OV, Pivovarov MM, Golubev SN, Konakov VG. Structure and conductivity of calcia stabilized zirconia ceramics, manufactured from freeze-dried nanopowder. *Rev Adv Mater Sci*. 2017;52(1-2):134-41.
28. Prasad RR, Yadav KL, Puri D, Daniel BS. Conductivity measurement of calcia stabilized zirconia prepared by mechanical route. *Adv Mat Res*. 2012;585:245-9.
29. Asadikiya M, Zhong Y. Oxygen ion mobility and conductivity prediction in cubic yttria stabilized zirconia single crystals. *J Mater Sci*. 2018;53(3):1699-709.
30. Chen C, Shen Q, Li J, Zhang L. Sintering and phase transformation of 7wt% calcia-stabilized zirconia ceramics. *J Wuhan Univ Technol Mater Sci Ed*. 2009;24(2):304-7.
31. Chen CL, Wang HQ, Ji JY, Luo MY, Wu B, Hu MW, et al. Preparation and electrical property of calcia stabilized zirconia ceramics. *Key Eng Mater*. 2014;616:157-65.
32. Kwon SY, Jung IH. Critical evaluation and thermodynamic optimization of the CaOZrO₂ and SiO₂-ZrO₂ systems. *J Eur Ceram Soc*. 2017;37(3):1105-16.
33. Piva RH, Piva DH, Souza MT, Morelli MR. Compatibility analyses of BICUVOX.10 as a cathode in yttria-stabilized zirconia electrolytes for usage in solid oxide fuel cells. *Mater Res*. 2014;17(5):1173-9.